Study on Behavior of Connection Mechanism on Hybrid-Rigid Frame Bridge Structure

Mochammad AFIFUDDIN*, Atsuhiko MACHIDA**,
Takao SUGIYAMA*** ,Toru SATO****

*M.Eng, Graduate School, Saitama University, 255 Shimo Okubo, Urawa 338, Saitama
**Professor, Dr.Eng, Dept.of Civil .Eng., Saitama University, 255 Shimo Okubo, Urawa 338, Saitama
***M.Eng, Japan Highway Coorporation, 4 Jyo-Nishi 5-1-3, Tyuou-ku, Sapporo 160, Hokaido
****Miyaji Iron Work Co., Ltd, Tokyo

The objectives of this paper are to study the behavior of connections of hybrid-rigid frame bridge structure, and to clarify the load transfer mechanism between element in the connection. Two types of specimens modeling the hybrid rigid frame bridge structure were tested under cyclic lateral loads. In designing the specimens, the stud shear connectors are chosen as main parameter. Moreover, the behaviors of stiffeners, reinforcing bars, and flange of girder were also examined. The load transfer mechanisms of tested specimens were presented in detail to provide some good information for understanding the behavior of the hybrid rigid frame structure under cyclic loading. It is concluded that in the specimen with stud shear connectors the stiffener will carry tension force larger than the specimen without stud shear connectors. On the other hand, the specimen without stud shear connectors will carry larger compression force than the specimen with stud shear connectors.

Key Words : *Hybrid-Rigid Bridge, Connection mechanism,Load transfer mechanism*

1. Introduction

In the field of bridge engineering, one possible method of connection between the reinforced concrete pier and the steel girder of the hybrid rigid-frame structure is by prestressing with post-tensioned tendons. Though this method of connection has reliable performance, the application to actual bridges is limited because of its rather complicated construction works and high construction cost. To solve such problems, an alternate method was developed without using prestressing in connecting the reinforced concrete pier and the steel girder. Steel-concrete hybrid rigid frame structure is a structural type where steel girder connects rigidly to RC column bridge without bearings. The seismic resistant of such structures will be enhanced and a light weight superstructure could be achieved. The reduction in weight of some sections could reduce the maintenance fee as well. However, there has been no studies up to now about the load transfer mechanism, and load carrying capacity of hybrid rigid structure. To the best of author's knowledge, the only similar study related to the strength and ductility of beam-to-column connections in hybrid bridges is the one carried out by Matsui et.al[1]. As such there is a necessity to investigate the behavior of such structures in detail. Finally, to propose a rational design for such connection, detailed investigation on the behavior of each member is considered.

The objectives of this paper are to study the behavior of connections of hybrid-rigid frame bridge structure, and to clarify the load transfer mechanism between element in the connection. The paper presents experimental result as well as analytical investigation for that structure. Two dimensional finite element model was used to conduct the analytical investigation for all specimens. Load carrying capacity of the specimens, load transfer from RC Column to steel girder, the behavior of stiffeners, stud shear connectors, flanges of girder are also presented and discussed in this paper. It is concluded that the role of studs in the stiffener are to distribute the

stress from stiffeners to concrete in compression side, and to transfer the stress from concrete to the stiffener in tension side. Also if no studs exist in the stiffeners, it was found that the stress concentrations occur in the upper part of flange.

2. Outline of Experiment

2.1 Specimens and Experimental Setup

The specimens consist of steel girder, reinforced concrete column, stiffeners, main reinforcements, and stud shear connectors. Stiffeners are fixed in steel girder, and main reinforcements are continuous from the reinforced concrete column to the steel girder through the holes in the upper flange. The reinforcements were anchored to the concrete within the space enclosed by upper and bottom placed of flange, web plate, and stiffeners. As such, the steel girder and reinforced concrete column are made to a single structure. The specimens will transfer compression force that is carried by the reinforcement in RC column. The shear forces transferred to the specimens depend on the stud shear connectors in the flange of steel girder, main reinforcements, and concrete. Figure 1 shows the detail of connection for each specimen. There are two types of specimens, S-type and T-type. In S-type, studs exist only in upperflange of steel girder or the intersection of the connection part of RC column and steel girder. On the other hand, in T-type, studs exist not only in the upper flange of the steel girder but also in the stiffeners of the connection part. The objective of T-type specimen is to determine the effect of stud shear connectors in the stiffener that may have ability to transfer some additional loads through the connection.

RC column has a section of 400 x 900 mm, and point load is applied on the top of RC column that is 1400 mm above the upper flange. Steel bars of diameter 25 mm are used as main reinforcement, with 2 layers at a spacing of 60 mm between the layers. Steel ratio for bar is 1.2 %. Bar of D13 is used as stirrups with a spacing 100 mm, the spacing is reduced to 50 mm in the area near the loading point. The stud shear connectors had a head diameter of 13 mm and the height being 80 mm. In the experiments, the specimens were fixed inversely compared to

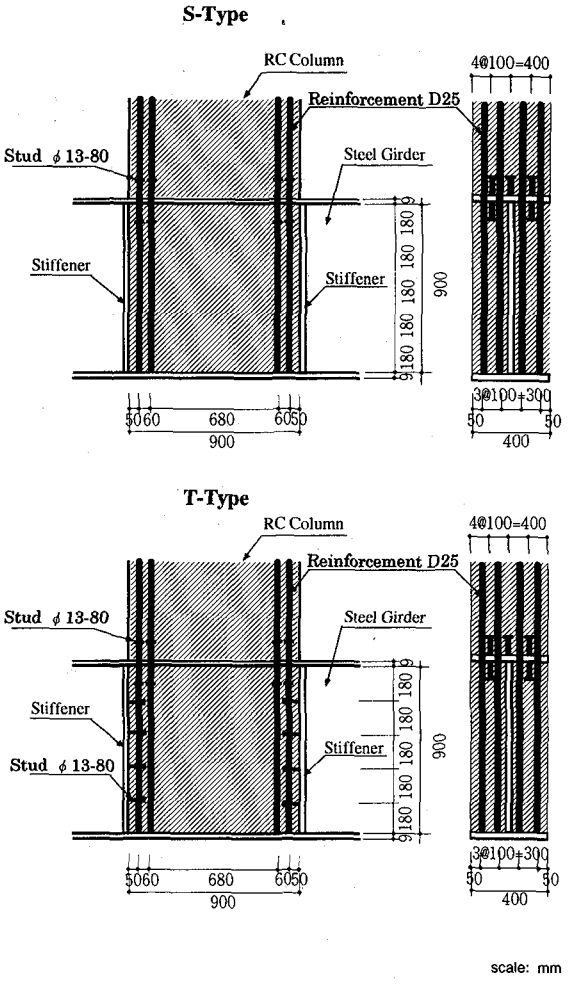

Fig. 1 Detail of each specimen

ordinary structures. The experimental setup is shown in Figure 2. The load applied at the top of reinforced concrete column, the data was measured from the strain gauge and displacement transducer attached to the specimen. In this paper, condition of each specimen based on the loading situation will be explained. The direction of actuators head is considered plus for tension load, and minus for compression load. Static half loading of crack occurrence, loading at crack occurrence, allowable stress of reinforcement, are checked during the applied load added in plus and minus direction alternatively. The loading pattern is shown in Figure 3.

2.2 Material Properties

Material properties used in this study are shown in Table 1.

Table 1 Properties of Material

Reinforcing bars	yielding stress (N/mm^2)	yielding strain (μ)	modulus elasticity ($\times 10^6$ N/mm^2)
SD345 D13	371.29	2320	0.16
SD345 D25	389.63	2171	0.18
Steel	yielding stress (N/mm^2)	tensile stress (N/mm^2)	elongation (%)
flange plate	296.27	449.85	29
Stud	yielding stress (N/mm^2)	yielding strain (μ)	tensile stress (N/mm^2)
ϕ13-80 mm	443.28	2300	521.54
Concrete	1 (N/mm^2)	2 (N/mm^2)	3 (N/mm^2)
S-type	33.09	30.78	25.60
T-type	32.26	33.46	33.23

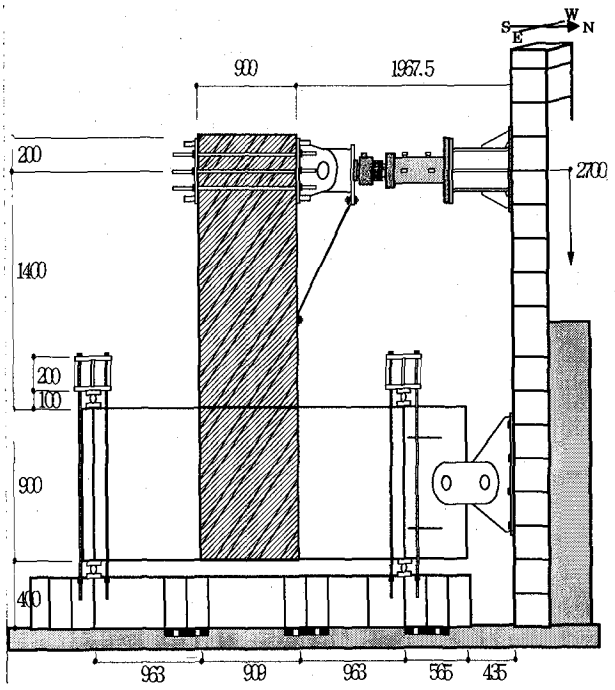

Fig. 2 Experimental Setup

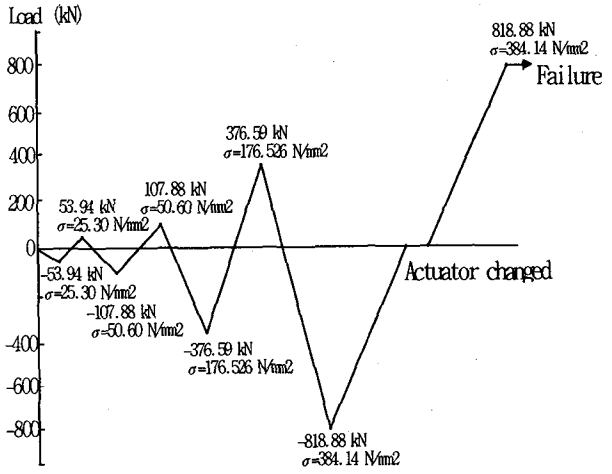

Fig. 3 Loading Pattern

3. Outline of Analysis

3.1 Material Modeling

The materials involved in this study are concrete, reinforcing bars, and steel plates. In the following section, the constitutive models used for each material will be described.

(1) Concrete

The intrinsic shape of the concrete stress-strain curves, for uniaxial and biaxial cases, is shown in Figure 4. This relation was proposed by Saenz[2]. The more detailed equation for stress degrading effect for concrete parallel to the crack surfaces is referred to paper written by Hsuan[3]. Under biaxial or combined stress fields, concrete is assumed to behave as a stress-induced orthotropic material. This implies that the initial tangent moduli in the two principal directions are different except for the case $\sigma_1/\sigma_2 = 1$, where σ_1 and σ_2 are the maximum and minimum principal stresses. The constitutive matrix, D, is

adopted from Darwin et.al[4)]

$$[D] = \frac{1}{1-\nu^2}\begin{bmatrix} C_{11} & C_{12} & 0 \\ C_{21} & C_{22} & 0 \\ 0 & 0 & C_{33} \end{bmatrix} \quad (1)$$

where:

$$C_{11} = E_1 \quad (2)$$

$$C_{12} = C_{21} = \nu\sqrt{E_1 E_2} \quad (3)$$

$$C_{22} = E_2 \quad (4)$$

$$C_{33} = (1/4)\left(E_1 + E_2 - 2\nu\sqrt{E_1 E_2}\right) \quad (5)$$

Cracking is monitored by checking the magnitude of σ_1 and σ_2. When the principal tensile stress at a point equals or exceeds the tensile strength of concrete, cracking is assumed perpendicular to the particular direction, then the matrix D reduces to Eq. 6.

$$[D] = \begin{bmatrix} 0 & 0 & 0 \\ 0 & E_t & 0 \\ 0 & 0 & \beta G \end{bmatrix} \quad (6)$$

$$E_t = \frac{df_c}{d\epsilon} = \frac{E_c[1+B-2C]}{[1+A-B-C]^2} \quad (7)$$

where:

$$f_c = \frac{E_c\epsilon}{1+A-B+C} \quad (8)$$

$$A = (R + R_E - 2)\left(\frac{\epsilon}{\epsilon_0}\right) \quad (9)$$

$$B = (2R-1)\left(\frac{\epsilon}{\epsilon_0}\right)^2 \quad (10)$$

$$C = R\left(\frac{\epsilon}{\epsilon_o}\right)^3 \quad (11)$$

in which:

$$R = \frac{R_E(R_\sigma - 1)}{(R_\epsilon - 1)^2} - \frac{1}{R_\epsilon} \quad (12)$$

$$R_E = \frac{E_c}{E_o} \quad (13)$$

$$R_\sigma = \frac{f_{cm}}{f_{cf}} \quad (14)$$

$$R_\epsilon = \frac{\epsilon_f}{\epsilon_o} \quad (15)$$

and

$$E_o = \frac{f_{cm}}{\epsilon_o} \quad (16)$$

Where G = elastic shear modulus and β = shear retention factor. The tangent modulus E_t used in Eq.6 can be calculated by differentiating f_c, and the result is shown in Eq.7. After deformation of the crack, concrete is also able to transfer tension between the cracks. In this study, the phenomenon is considered by assuming a descending branch for the concrete in tension, as shown in Figure 4. After the formation of the cracks at a given point, concrete can still carry some tension up to a maximum tensile strain of $10\epsilon_{cr}$, where ϵ_{cr} is cracking strain, but it is assumed to have zero stiffness normal to the direction of the crack.

(2) Reinforcing Bars and Steel Plate

Reinforcing bars and steel plate are modeled as an elasto-plastic material, as shown in Figure 5. The material parameters, f_y, E_s , and ϵ_u are the yield stress, Young's modulus, and ultimate strain that need to be input to define the relationship.

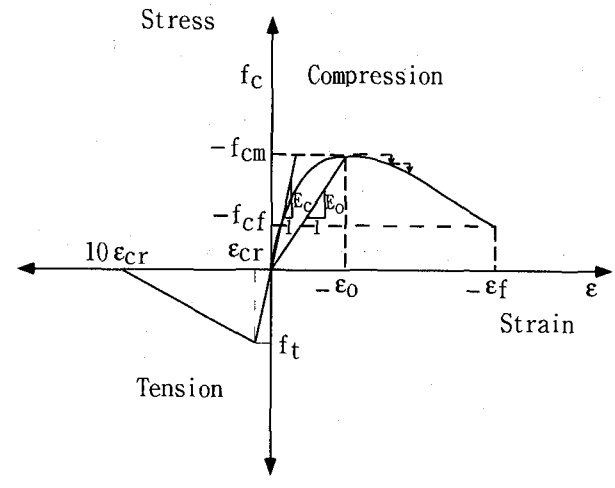

Fig. 4 Constitutive Equation for Concrete

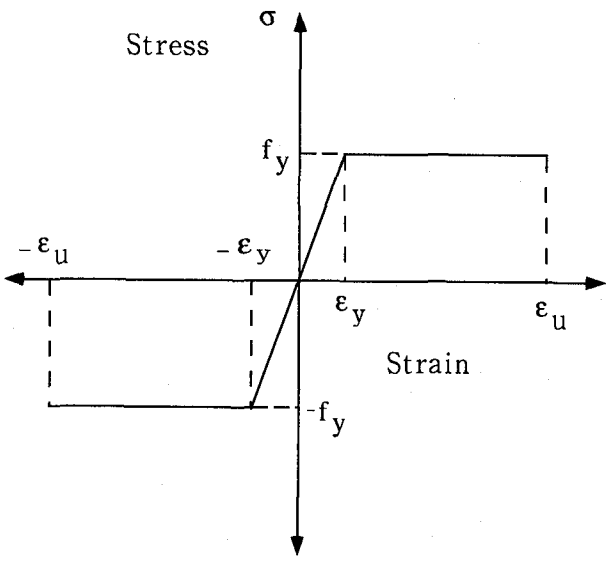

Fig. 5 Constitutive Equation for Steel

(3) Local Bond Stress-Slip Relationship

Bond stress-slip relationship adopted from model proposed by Shima[7]. The local stress at any location along an embedded bar is thus proporsional to the slope of the strain distribution curve at that point. At any point, the bond stress, τ, is expressed as:

$$\tau = \frac{E.Dd\epsilon}{4dx} \qquad (17)$$

where E is the Young's modulus of the bar. D is the bar diameter and $d\epsilon/dx$ is the slope of the strain distribution curve.

The local slip, S, was determined by integrating the strain over the length of the rebar starting from the midway between adjacent cracks.

$$S = \int_0^x \epsilon dx \qquad (18)$$

3.2 Analytical Program

The structures are analyzed by using the Finite Element program MARC[5]. The structures are divided into several elements. The dimensions and the mesh of each element are shown in Figure 6. Plane stress element having 8 nodes was used for modeling the concrete and steel plate, and truss element was used for modeling steel reinforcement and stud shear connector. The model for S-type consists of 136 elements of web plate, 48 element stiffeners, 100 elements of concrete, 60 elements of reinforcing bar, and 8 elements of shear connector. The only difference between the S-type and T-type model was the number of shear connector being 16 elements of shear connector in T-type. The connection between stiffener and web plate was assumed to be fixed. Boundary conditions for numerical analysis, 12 nodes are pin, and 1 node is fixed. The thickness of concrete column was 400 mm. Area of steel reinforcement was 7853.98 mm^2. Material properties used in analytical work was same like in experimental work as shown in Table 1. The analysis was performed by applying the cyclic loading that has similar pattern with the experimental work[6] as shown in Figure 3. Strains and stresses of each integration point in every element were printed in each load increment, and the deformation was determined. The Modified Newton-Raphson method was adopted in the iteration scheme in current nonlinear analysis.

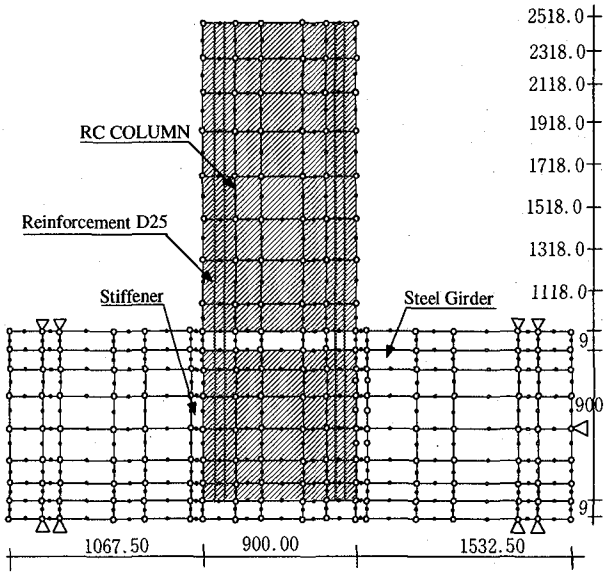

Fig. 6 Mesh Generation of Specimen

4. Experimental and Analytical Result

4.1 Load Carrying Capacity of the Specimens

Table 2 shows the comparison of analytical and experimental results for both S-type and T-type. Plane crack occurred in RC column connection part in each specimen when the load was about 98.07 kN. With increasing load, the crack width

Table 2 Comparison of Analytical and Experimental Result

Action	Analytical(kN)		Experimental(kN)		Anal./Exp.	
	S	T	S	T	S	T
First crack in concrete	112.78	121.61	98.07	98.07	1.150	1.250
First yield of RC-1	759.06	753.18	745.33	735.53	1.020	1.024
First yield of RC-2	835.56	838.50	823.79	845.36	1.014	0.992
Complete cracking	872.82	884.59	863.02	870.86	1.011	1.016
Failure load	922.84	896.36	914.99	889.50	1.010	1.008

became larger and propagated further into the section. However, fatal destruction did not occur at this position, because in connection part the stress was transferred through the main reinforcement and studs in the flange. Figure 7 shows the opening between RC column and steel girder in tension side. The yielding of reinforcing bars at the top flange and at the point 190 mm above the top flange are denoted by points a and b respectively. Even though the RC column did not show substantial increase in load carrying capacity after yielding, the large destruction did not occur. After yielding took place at point b, the increase in load was negligible. The loads are 825.75 kN for S-type, and 845.36 kN for T-type respectively. Load carrying capacity of the specimens does not increase after diagonal crack occurs in concrete connection part. From the above discussion, it can be said that the connection of this form is suitable for concrete column-steel girder hybrid structures.

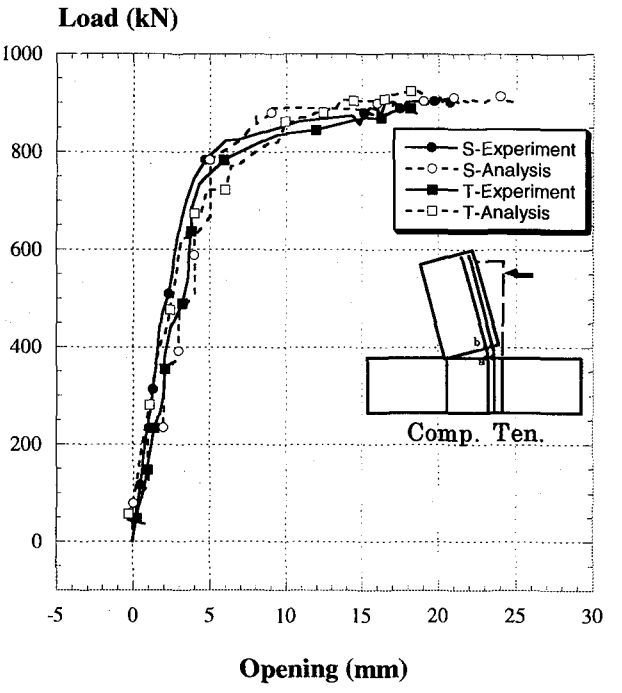

Fig. 7 Opening between RC Column and Steel Girder

4.2 Load Transfer from RC Column to Steel Girder

Figure 8 shows relationship between the average bond stress and load. This was obtained by integrating the bond stress in reinforcement located in connection part and dividing it by the length of the reinforcement. The bond stress was calculated by using the method proposed by Shima[7]. The same figure shows the design bond stress per unit area and the yielding load for reinforcement at top flange of steel girder. The design bond stress value is 2.64 N/mm^2. The design bond stress is used for obtaining the anchorage length of reinforcement in JSCE standard specification for design and construction of concrete structure[8]. The solid line in the figure shows the position of calculated anchorage length of reinforcement assuming the full length is effective in connection part. In S-type, the empirical values lie almost in a straight line. On the other hand, because the bond stress of reinforcement becomes large, the empirical values of T-type give results on the unsafe side. In T-type, vertical cracks occurred in connection part of concrete in the last loading cycles. Even if the stress is transferred in connection part, if transverse reinforcement is not enough, load carrying capacity does not work well. The dotted line in the figure shows the average bond stresses in case anchorage length increased by half the effective

height. It could be understood from these result that in T-type; the necessary anchorage length of reinforcement might have to be increased by more than half of the effective height. It is in addition to the calculated length basic anchorage legth specified in JSCE standard specification for design and construction of concrete structure[8].

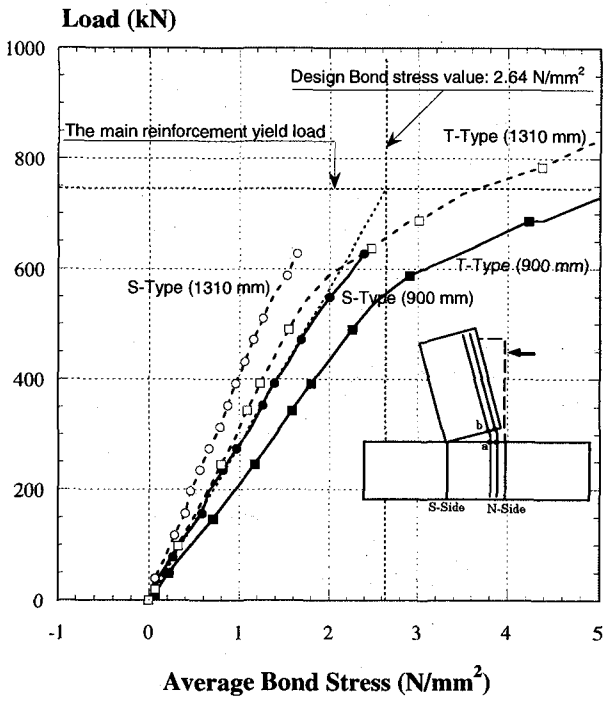

Fig. 8 Average Bond Stress and Load Relationship

4.3 Behavior of the Stiffeners

The distribution of compression force and tension force in the stiffener was investigated. From the numerical results, the model can predict the results closely as can be seen from the comparison with the experimental result. All the results are shown in Figure 9 and 10, and point a-b-c-d are used as an investigation point. It can be seen from the figures that S-type specimen carries more compression force than T-type. On the other hand, T-type specimen carries more tension force than S-type. It can be investigated from the experimental work that when compression load applied to the specimen, in the tension region, the reinforcing bars carry the tension forces. Through the bonding between concrete and reinforcing bars, the force transferred smoothly to stud shear connectors, and finally the force transferred to the stiffeners. On the other hand, in the compression region, the load directly transferred to stiffener, then transferred to stud shear connectors, and finally transfer to concrete. In S-type case, where there are no stud shear connectors exist in the stiffener, the compression force was transferred directly from the stiffener to the flange of girder. On the other hand, tension force transferred through the bonding between concrete and reinforcing bars to the flange of the girder. The maximum tension and compression force that can be carried by the stiffener are about 333.44 kN. In T-type, for upper part (ab), the tension force increases gradually and then drop suddenly at the load level of 686.49 kN, and the force is larger than the S-type. The reason is as an effect of crack opening in connection part; the compression zone area is become decrease. On the other hand, the compression force for S-type is larger than that of T-type. The phenomena mention above also appears on the behavior of lower part of stiffener (cd) in tension and compression force results.

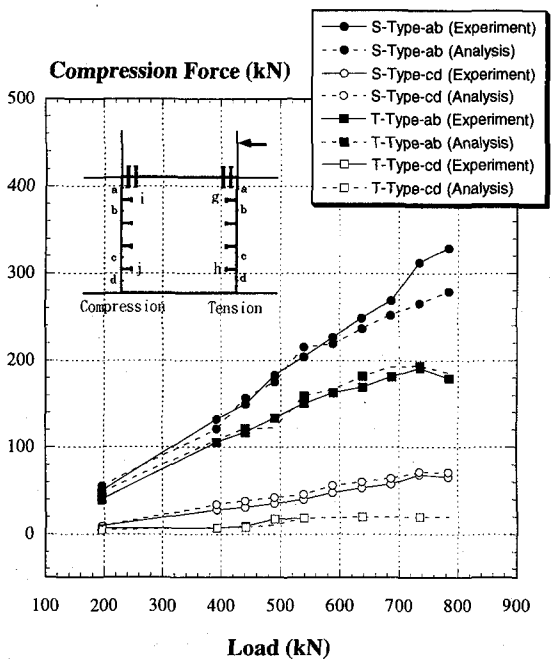

Fig. 9 Load Compression Force Relationship in the Stiffener

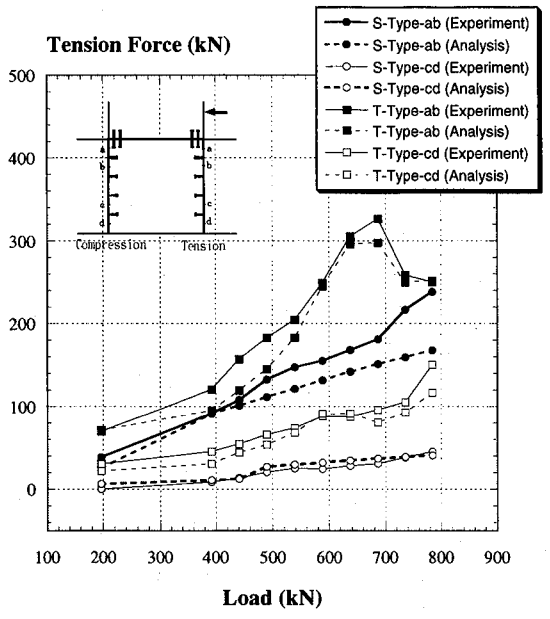

Fig. 10 Load Tension Force Relationship in the Stiffener

4.4 Behavior of Studs

Figure 11 and 12 show the comparison result for compression force transferred to concrete by stud shear connector. On the other hand, Figure 13 and 14 show the comparison result for tension force transferred to concrete by stud shear connector. In this study, we use two ways, A and B, to investigate the load carried by stud shear connectors. In method A, load carried by stud shear connectors are calculated from the difference of strain in ab (or cd) multiplied by modulus of elasticity and cross section area of stud shear connectors. While, in method B, the load is calculated based on the average strain in ab (or cd) of each specimen multiplied by modulus of elasticity and cross sectional area of studs. It can be seen from the figures that difference phenomenon occurs in studs i and j for compression force. On the other hand, the same patterns also appear in studs g and h for tension force. It show in the Figures that when the applied load is less than 686.49 kN, A carried the tension force more than B, but when the applied load is more than 686.49 kN, B gets more compression force than A. The reason is after applied loads reach 686.49 kN, the main reinforcing bars reach to the yield condition. It will affected the transfer load in the studs shear connectors. Due to cracking in the connection part, the area of concrete in that part becomes reduce, and it can reduce the transferred force from concrete to the stiffener, so method B got more compression force than method A. It can be concluded that if studs are placed in compression side of the stiffeners, the stiffener will carry small compression stress, because compression stresses are distributed in connection part of concrete through stud shear connectors. In tension side, it is clear that tension stress transferred to the stiffeners becomes large, because in connection part concrete transfers tensile stress to the stiffeners from stud shear connectors. So the studs in this position affects the load transferring in connection part between concrete and stiffeners.

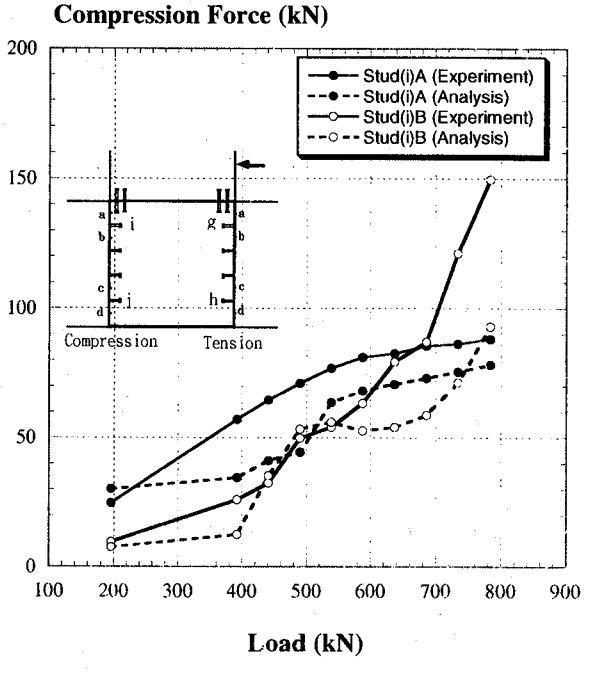

Fig. 11 Compression Force transferred to concrete by studs shear connectors

4.5 Behavior of the Flanges

Behavior of flanges was monitored by checking the strain distribution outside the flange. Comparison results for upper and bottom part of S-type are presented in Figures 15 and 16, and Figures 17 and 18 present the comparison results for upper and bottom part of T-type, respectively. From the figures, we can see that the numerical investigation have good agreement with the ex-

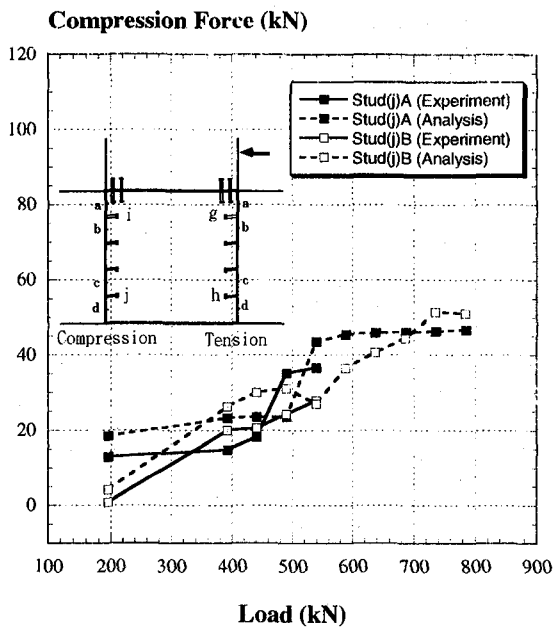

Fig. 12 Compression Force transferred to concrete by studs shear connectors

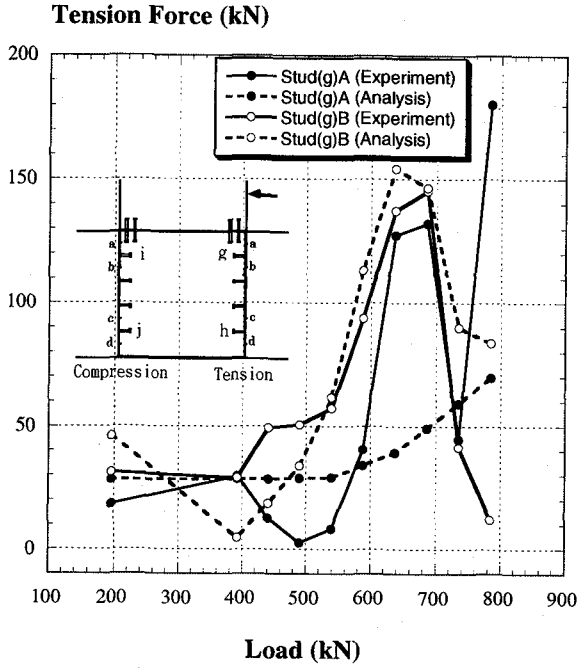

Fig. 13 Tension Force transferred to concrete by studs shear connectors

perimental investigation. In S-type, upper part of tension side, the result is larger than T-type. On the other hand, in the other side, the result is not so big different between S-type and T-type. When we take a look at bottom part of each type, both of them show the strain in compression side is larger than the strain in tension side. This be-

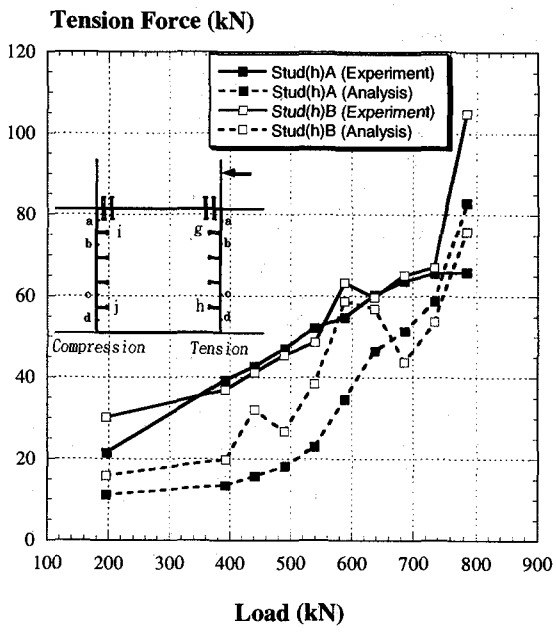

Fig. 14 Tension Force transferred to concrete by studs shear connectors

havior can be easily understood that when the stud shear connectors exist in the stiffener, the force will transferred to the studs and stiffener. On the other hand, when the studs do not exist, the force will transfer from the concrete column not only to stiffener through bonding between reinforcing bars and concrete, but also to the flange.

4.6 Discussion

The effectiveness of the location of stud in the stiffeners for compression and tension side is shown in Figures 19 and 20 respectively, by plotting the ratio of transferred load on cd and ab. In early stages of loading this ratio is 40 % at tension side of T-type. However, in the final stage of loading, this ratio is only about 10-20 %. This shows the rate of stress transferred to stiffener in bottom side is generally smaller compared to top side. As such, it is concluded that the studs located in top side of stiffeners work effectively in transferring the stress between connection part and stiffeners at early stage of loading, but in the final stage load the behavior is afterward. Figure 21 shows the load transfer mechanism for S-type and T-type specimen. In compression of S-type, greater part of the load will be transferred directly to the stiffener through connec-

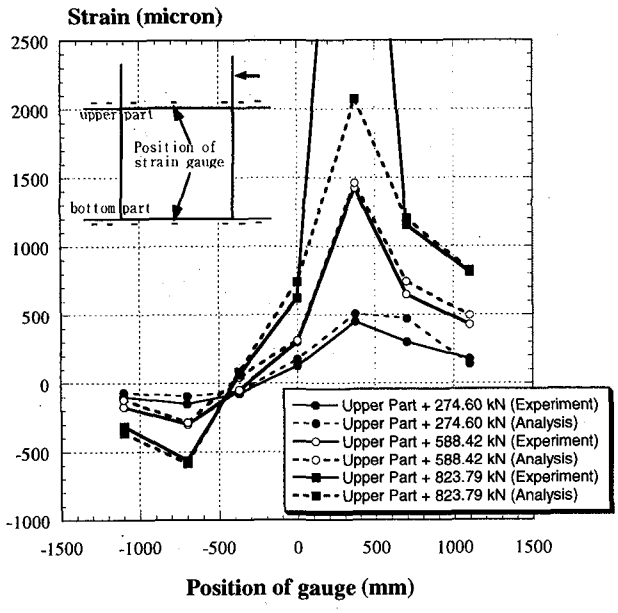

Fig. 15 Strain Distribution on upper flange of S-Type

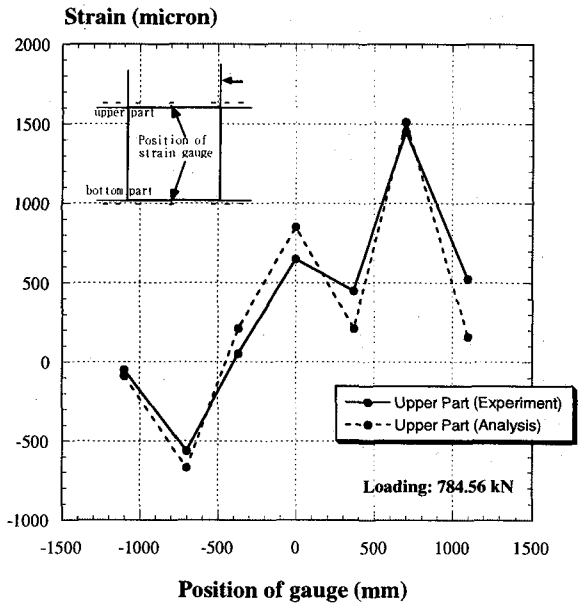

Fig. 17 Strain Distribution on upper flange of T-Type

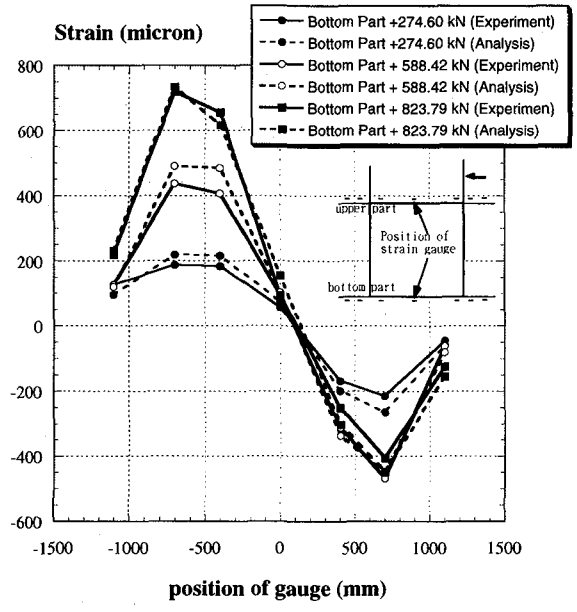

Fig. 16 Strain Distribution on bottom flange of S-Type

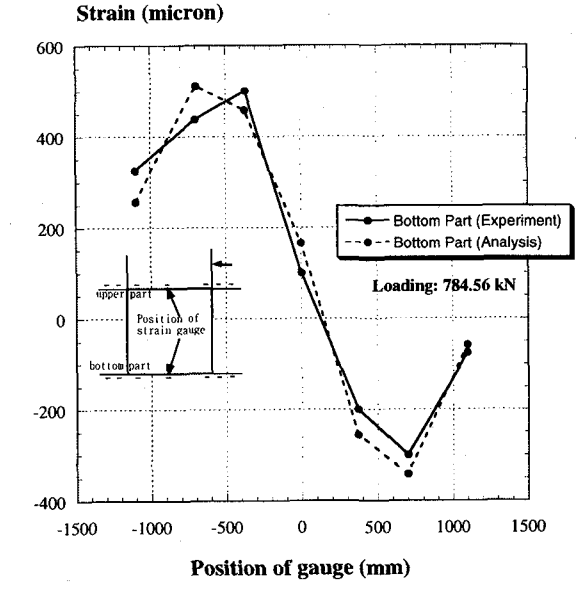

Fig. 18 Strain Distribution on bottom flange of T-Type

tion between concrete column and steel girder. On the other hand, in tension side the load will not be transferred to the stiffener through bonding between reinforcing bars and concrete in connection part. Also we can see that the strain distribution on the upper part of flange is large due to tension force which transfer through the concrete to the flange. The stain distribution on the bottom part of flange in compression side also large due to the load transferred from the stiffener. All this phenomenon has been shown in the previous figures.

Concerning about T-type specimen, the behavior of compression side when the compression

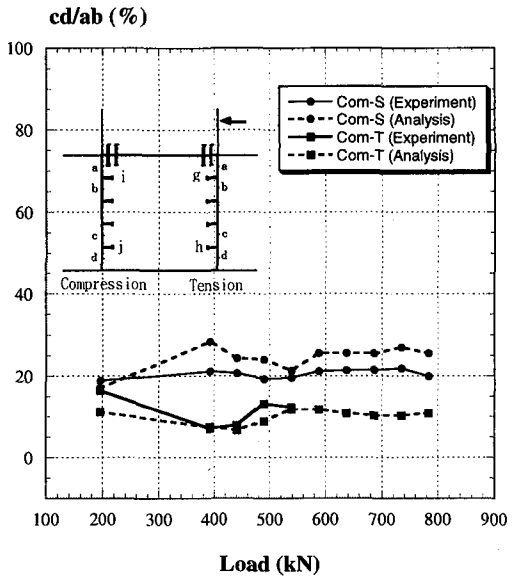

Fig. 19 The ratio transferred load on cd and ab in compression zone

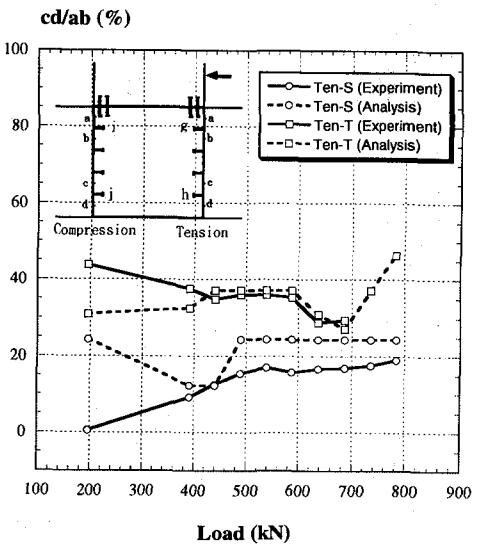

Fig. 20 The ratio transferred load on cd and ab in tension zone

force applied to the specimen, the load will transfer directly to the stiffener. Then the load will be distributed to studs shear connectors that is exist in the stiffener. Also from the studs, the load will transfer smoothly to concrete in connection part. In tension side, the load will transfer from bonding between concrete and reinforcing bars to the stud shear connectors. Then the load will be transferred to stiffener, and the flange of girder.

5. Conclusions

The results obtained in this study are summarized below:

(1) The rigidities of the specimens were still maintained even after the reinforcement reached the yield point in the upper part of flange. It was found that the connection makes an almost rigid connection and is of the appropriate form.

(2) Anchorage length of reinforcement must be provided such that the average bond stress does not exceed the allowable limits.

(3) The role of studs in the stiffener is to distribute the stress from stiffeners to concrete in compression side, and to transfer the stress from concrete to the stiffener in tension side.

(4) If no studs exist in the stiffeners, it was found that stress concentration occur in the upper part of flange.

(5) The top side of stiffeners undergo very large strain, and the studs in the stiffeners play an effective role in transferring the stress.

References

1) Matsui S., Yukawa Y., Wada N., Ishizaki S., and Tanaka T.; "Strength and Ductility of Beam-to-Column Connections in Hybrid Bridge", Conference Report on Composite Construction-Conventional and Innovative, pp.469-474, IABSE, September 1997.

2) Saenz, L.D.;"Discussion of equation for the stress-strain curve of concrete by Desayi and Khrishnan" ACI Journal Vol.61 No.9, 1964.

3) Hsuan-Teh Hu., and William C. Schnobrich;"Nonlinear Analysis of Cracked Reinforced Concrete". ACI Journal Vol.87 No.2, 1990.

4) Darwin, D., and Pecknold, D.A.; "Nonlinear biaxial stress-strain law for concrete,". J. Struct. Engrg. ASCE Vol. 103 No.4 1974.

5) Marc Analysis Research Corporation.; "Marc Manual, Vol: A - E",1997

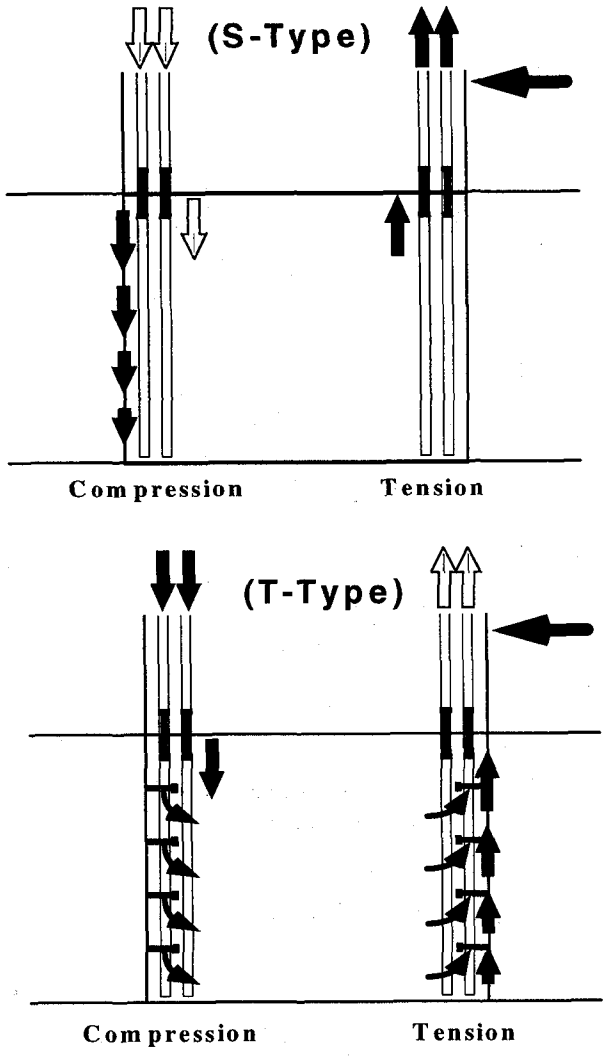

Fig. 21 Load Transfer Mechanism of Each Types

6) Takao Sugiyama, Afifuddin Mochammad, et.al.; "A Study on Connection Mechanism of T-joint in Steel-Concrete Hybrid Rigid Frame" Proceeding JCIVol.19, June, 1997.
7) Shima H., Chou L., and Okamura, H.; "Bond-Slip-Strain Relationship of Deformed Bars Embedded in Massive Concrete" Journal of Materials, Concrete Structures and Pavements, No: 378/ V-6, pp. 165-174, JSCE, February 1987.
8) JSCE Commitee on Standard Specification for Design and Construction of Concrete Structures,; "Standard Specification for Design and Construction of Concrete Structures, Part 1 (Design)", JSCE, 1986.

(Received September 26, 1997)